PROCEEDINGS OF SCIENCE

QCD Axion Emission from Higher-Generation Matter in Core-Collapse Supernovae

Diego Guadagnoli[a,*]
[a] *LAPTh, Université Savoie Mont-Blanc et CNRS, Annecy, France*
E-mail: diego.guadagnoli@lapth.cnrs.fr

We present an effective-field-theory calculation of QCD axion emissivity from dense matter beyond the first quark generation in the context of core-collapse supernovae. By including the full meson and baryon octets, we evaluate all additive contributions from 134 Compton-like processes $B_i M \to B_f a$, with B octet baryons and M octet mesons, as well as 7 baryon decays $B_i \to B_f a$, obtaining robust order-of-magnitude bounds on various axial couplings of the axion to light quarks i, j, $(\boldsymbol{k}_A)_{ij}$. Our results reveal strong correlations among diagonal axial couplings $((\boldsymbol{k}_A)_{11}, (\boldsymbol{k}_A)_{22}, (\boldsymbol{k}_A)_{33})$ and provide stringent direct constraints on flavour violation induced by the axial a-d-s coupling: $|(\boldsymbol{k}_A)_{23}| \lesssim 10^{-1} - 10^{-2}$. The material presented here is based on Ref. [1].

Preprint: LAPTH-Conf-051/25

The European Physical Society Conference on High Energy Physics (EPS-HEP2025)
7–11 July 2025
Marseille, France

*Speaker

https://pos.sissa.it/

PoS(EPS-HEP2025)105

1. Motivation

In this work we discuss axion emission from matter beyond the first generation in core-collapse supernovae (SNe). The key questions we attempt to address are how important higher-generation hadrons, in particular with strangeness, are for axion emission; and what the SN 1987A signal implies for axion couplings involving the strange quark.

Here, when speaking about the axion, we focus on the QCD axion. The latter arises from a spontaneously broken Peccei–Quinn symmetry at a very high scale f_a, and its mass m_a is inversely related to f_a. For the range of f_a of interest, this implies a very small mass, at the level of a few meV or below. The QCD axion is thus a "light interloper from a high-energy world" in the sense of Ref. [2]. At low energies, axion interactions with matter are amenable to a rigorous effective description within low-energy QCD, i.e. chiral perturbation theory (ChPT) [2]. The axion couples derivatively to matter, through terms of the schematic form

$$\mathcal{L}_{aqq} = \frac{\partial_\mu a}{f_a} \left(\bar{q}\, \gamma^\mu_L \mathbf{k}_L\, q + \bar{q}\, \gamma^\mu_R \mathbf{k}_R\, q \right) , \tag{1}$$

with $q = (u, d, s)^T$ and where the hadronic realization of the left- and right-handed currents is given in terms of octet meson and octet baryon fields. The corresponding couplings are calculable within ChPT and can be expressed as linear functions of the fundamental matrices $\mathbf{k}_{L,R}$.

Given the derivative structure, the effective coupling strength scales as external momenta over f_a. For laboratory processes, momenta are vastly below f_a, and this generally implies tiny couplings. Dense and hot astrophysical objects are therefore particularly promising: if they are hot and dense enough, they may radiate axions efficiently and cool faster than expected from neutrino cooling alone. Core-collapse SNe, within the standard picture that remains relatively calculable, stand out as probes of the QCD axion [3, 4].

2. The Raffelt bound and axion emissivity

The key observable that constrains axions is the neutrino burst from SN 1987A. The measured signal is compatible with expectations from standard neutrino cooling within sizeable, but finite, theoretical uncertainties. This compatibility leaves limited room for exotic energy-loss channels and leads to the classic *Raffelt bound* [3] $Q_a \; < \; Q_\nu$, where Q_a is the emissivity (power per unit volume) in axions and Q_ν the corresponding quantity for neutrinos. This is the basic inequality we will use. The axion emissivity Q_a is a calculable quantity. For a given process in the medium that produces an axion, one has

$$Q_a \; = \int E_a \, (2\pi)^4 \delta^{(4)}(p) \, |\mathcal{M}|^2 \prod_j \frac{d^3 p_j}{(2\pi)^3 2E_j} \, f_j \, (1 \mp f_j) \, , \tag{2}$$

where E_a is the axion energy; $\mathcal{M}$ is the matrix element for the axion-producing process; f_j are the distribution functions of the external states in the hot, dense medium; the "$\mp$" accounts for Fermi blocking or Bose enhancement. This expression applies both to scattering reactions and, with obvious modifications, to decays.

The evaluation of Q_a requires assumptions. The distribution functions of the external states are not obvious beyond the ideal-gas approximation, which is inherent in the explicit formula for the f functions. One may take a mean-field approach, where chemical potentials, single-particle energies and effective masses account for interactions in a dense medium, and are accordingly replaced by their in-medium counterparts.

On the right-hand side of the Raffelt bound, Q_ν cannot be computed to better than order-of-magnitude accuracy. A standard estimate is $Q_\nu \sim L_{\rm SN}/V_{\rm core} \sim L_{\rm SN}/M_{\rm core}\,\rho$, where the luminosity $L_{\rm SN}$ is taken to be roughly half of the Newtonian binding energy, yielding $L_{\rm SN} \sim 3 \times 10^{52}$ erg/s, and $M_{\rm core} \sim 1\,M_\odot$ is a characteristic core mass. The resulting Q_ν is usually re-expressed in terms of the core density, which is itself uncertain. In short, the Raffelt bound is an *order-of-magnitude* constraint, but a robust one across a broad class of models [3, 4].

The matrix elements entering Q_a are currently understood primarily in terms of two classes of processes. The most established bound [3, 4] has long been derived from so-called nucleon axion-strahlung, $NN \to NNa$ [5], where N denotes a nucleon. More recent work has highlighted the importance of Compton-like processes such as $\pi N \to Na$, which may even dominate axion emission in some regimes [6]. Up to this point, however, most studies either focus on first-generation matter or include only a few specific hyperon channels [7].

This motivates the question that we address here: the impact of *beyond-first-generation* matter, in particular strange baryons, on axion emission and on the resulting SN 1987A bounds.

3. Full octet processes and strange matter

To address this question, we consider the full meson and baryon octets and compute all processes of the form $B_i M \to B_f a$ as well as $B_i \to B_f a$, with B an octet baryon and M an octet meson. The first class corresponds to Compton-like processes, and amounts to 134 channels in total. The second class contains 7 baryon decays. Together, they provide a complete description of axion emission from the octet sector at the level of our EFT.

Each of these channels contributes a separate, positive-definite term to Q_a. Their squared amplitudes do not interfere with one another in the emissivity, so all contributions are simply additive. This is crucial: even if the fractional number densities of B_i, B_f and M are small, say below 10^{-2}, the large number of available channels can still lead to a sizeable total Q_a. In other words, there is a combinatorial enhancement of the strange sector.

Our conclusions must be robust with respect to two aspects of modelling: the description of the axion-emitting volume in the SN core; the treatment of axion–matter interactions.

The state of matter in the core is specified by three thermodynamic parameters, which may be chosen as the temperature T, the baryon density n_B, and the electron fraction Y_e. We vary all of these quantities to probe the sensitivity of Q_a to each of them. Concretely, we scan $T = \{30, 40\}$ MeV, $n_B = \{1, 1.5\}\, n_{\rm sat}$, with $n_{\rm sat}$ the nuclear saturation density, and fix a characteristic total baryonic charge fraction $Y_{Q_B} \simeq 0.3$. Since nucleons dominate the baryon number, this implies a proton fraction $Y_p \simeq 0.3$, and, by charge neutrality, an electron fraction $Y_e \simeq 0.3$ in the absence of muons, in line with previous supernova axion studies.

To explore the impact of strange matter we employ two modern EoS models with the full baryon octet: the DD2Y and the SFHoY model [8, 9]. Both are compatible with nuclear and astrophysical constraints, but predict different hyperon abundances and therefore different strangeness fractions at fixed (T, n_B, Y_{Q_B}). Mesons are treated as an ideal Bose gas with chemical potentials fixed by the EoS and by charge neutrality, $Y_{Q_B} + Y_{Q_M} + Y_e = 0$. At a given thermodynamic point and for a given EoS, this setup determines the particle fractions and in-medium single-particle properties entering Q_a. In particular, effective masses, chemical potentials and mean-field potentials enter both the distribution functions and the energy-conservation delta function in the emissivity.

4. Axion–hadron EFT and which couplings are probed

The axion is derivatively coupled to left- and right-handed vector currents of light quarks u, d, s, encoded in the 3×3 matrices $\mathbf{k}_{L,R}$ in the same, light-flavour space. Below the hadronization scale, one changes degrees of freedom from quarks to hadrons. The quark-level Lagrangian, Eq. (1), is matched onto an effective theory written in terms of the axion field a, the octet meson field U and the octet baryon field B. It is convenient to work in terms of vector and axial combinations $\mathbf{k}_{V,A} = \mathbf{k}_R \pm \mathbf{k}_L$. In the hadronic EFT, the axion couples to left- and right-handed hadronic currents $\mathcal{J}^{b\mu}_{L,R}(U, B)$, labelled by an adjoint SU(3) index b. The effective Lagrangian can be written schematically as

$$\mathcal{L}_{aUB} = \frac{\partial_\mu a}{f_a} \sum_{b=1}^{8} \left[x_L^b \, \mathcal{J}_L^{b\mu}(U, B) + x_R^b \, \mathcal{J}_R^{b\mu}(U, B) \right], \tag{3}$$

where the coefficients $x^b_{L,R}$ are linear functions of the fundamental quark-level couplings $\mathbf{k}_{L,R}$. From this Lagrangian one derives the baryon–meson–axion and baryon–baryon–axion vertices used to construct the matrix elements for all processes entering Q_a.

For axion emission from SNe, the dominant sensitivity is to a restricted subset of the axial couplings, $(\boldsymbol{k}_A)_{11}$, $(\boldsymbol{k}_A)_{22}$, $(\boldsymbol{k}_A)_{33}$, $(\boldsymbol{k}_A)_{23}$, $(\boldsymbol{k}_A)_{32}$, where flavour indices label u, d, s. Electric-charge conservation implies that 12 and 13 off-diagonal entries are zero. Hermiticity implies that the diagonal entries are real, whereas $(\boldsymbol{k}_A)_{23}$ and $(\boldsymbol{k}_A)_{32}$ are complex conjugates.

Independent data already constrain some of these parameters. Neutron-star cooling bounds combinations of $(\boldsymbol{k}_A)_{11}$ and $(\boldsymbol{k}_A)_{22}$ [10], while kaon observables and hyperon decays constrain $(\boldsymbol{k}_{V,A})_{23}$ [7]. In our analysis we take a deliberately agnostic stance on the flavour structure. We treat the relevant entries of $\mathbf{k}_A$ as free parameters sampled over broad ranges, subject only to existing bounds from neutron-star cooling and kaon physics [7, 10]. The SN emissivity constraint $Q_a < Q_\nu$ is then applied on top of these, and we examine how much it further restricts the parameter space.

In short, axion emissivity from SNe primarily constrains the diagonal axial couplings $(\boldsymbol{k}_A)_{11}$, $(\boldsymbol{k}_A)_{22}$, $(\boldsymbol{k}_A)_{33}$, and the absolute value of the flavour-violating coupling $|(\boldsymbol{k}_A)_{23}|$.

5. Results: correlations and bounds on axion couplings

The constraints from our scan are conveniently visualized as matrix plots where each coupling, $(\boldsymbol{k}_A)_{11}$, $(\boldsymbol{k}_A)_{22}$, $(\boldsymbol{k}_A)_{33}$, $|(\boldsymbol{k}_A)_{23}|$, is shown against each of the others, see Fig. 1. We consider four benchmark thermodynamic points in T vs. n_B, namely {30, 40} MeV × {1, 1.5} $n_{\rm sat}$. For each

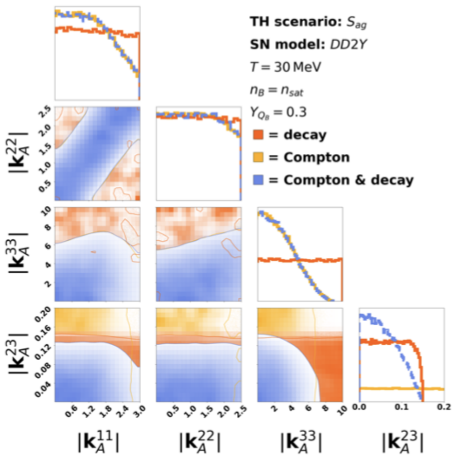

	$n_B = n_{\rm sat}$		$n_B = 1.5 n_{\rm sat}$	
$\boldsymbol{k}$ coupling	30 MeV	40 MeV	30 MeV	40 MeV
$\lvert(\boldsymbol{k}_A)_{23}\rvert$	0.35 **0.15**	0.12 **0.061**	0.38 **0.097**	0.14 **0.052**
$\lvert(\boldsymbol{k}_A)_{33}\rvert$	8.8 **8.9**	4.4 **4.8**	5.9 **3.9**	3.1 **2.9**

Figure 1: Left: Bounds on $|(\mathbf{k}_A)_{ij}|$ for $ij = \{11, 22, 33, 23\}$ from Compton-like reactions (yellow), decays (orange), and their sum (blue). Top-diagonal subplots: 1D posteriors; off-diagonal contours: 95% marginalized 2D regions. EoS: `DD2Y`, $Y_{Q_B} = 0.3$. Right: Summary of bounds on $(\boldsymbol{k}_A)_{23,33}$.

point we separate the impact of different classes of processes: the constraint from decays alone; the constraint from Compton-like processes alone; and the combined constraint from both classes.

The main take-aways from these plots are: *(i)* SN 1987A implies clear correlations between the diagonal axial couplings $(\boldsymbol{k}_A)_{11}$, $(\boldsymbol{k}_A)_{22}$ and $(\boldsymbol{k}_A)_{33}$. In particular, the coupling to the strange quark becomes correlated with those to the up and down quarks, which in turn are directly constrained by neutron-star cooling [10]. *(ii)* We obtain a direct constraint on the flavour-violating coupling $(\boldsymbol{k}_A)_{23}$, which can be as strong as $|(\boldsymbol{k}_A)_{23}| \sim 10^{-1}$–$10^{-2}$ ($f_a = 10^9$ GeV), depending on the thermodynamic point and on the EoS. Correlations tighten as T increases, reflecting the enlarged phase space and higher abundances of pions and hyperons at higher temperature. The bound on the coupling to the strange quark, $(\boldsymbol{k}_A)_{33}$, is dominated by Compton-like processes, whereas the constraint on $(\boldsymbol{k}_A)_{23}$ is primarily driven by hyperon decays, with Compton channels becoming increasingly relevant as T grows [4, 6, 7]. The bounds are summarized numerically in the table to the right of Fig. 1 for the two couplings that are directly constrained by SNe, namely $(\boldsymbol{k}_A)_{23,33}$. The table assumes $f_a = 10^9$ GeV. Bounds for a different f_a assumption can be simply obtained by recalling that, if $f_a \to f_a/x_f$, $Q_a \to Q_a x_f^2$ [1]. The larger boldfaced vs. smaller value quoted in each table entry refers to the EoS model being considered, `DD2Y` [8] vs. `SFHoY` [9].

6. Main messages and outlook

Let us conclude by summarizing the main messages. *(a.)* Core-collapse SNe and other compact objects are powerful probes of fundamental and well-motivated BSM physics, such as the QCD axion [3, 4, 10]. In this work we have deliberately focused on the QCD axion, as opposed to generic axion-like particles. *(b.)* Supernovae probe not only axion interactions with ordinary (first-generation) matter, but also couplings to higher-generation hadronic matter. Strange baryons and mesons, even when present at the percent level, can have a sizeable impact on axion emissivity once all octet processes are consistently included. *(c.)* Improved understanding of the sources is crucial to go beyond order-of-magnitude answers. On the astrophysical side, this calls for embedding axion emissivities into full hydrodynamical simulations including axion transport, and for a refined treatment of the EoS and strangeness content [8, 9]. On the theory side, it would be interesting to combine the bounds derived here with specific flavour models for axion couplings, such as KSVZ- or DFSZ-type completions, or frameworks with minimal flavour violation.

Finally, extending the present analysis to other compact objects, such as hyperon-rich neutron stars, may shed further light on axion interactions with strange matter and on the interplay between QCD dynamics and new physics in extreme environments [8–10].

Acknowledgment— I would like to thank my collaborators Maël Cavan-Piton, Micaela Oertel, Hyeonseok Seong and Ludovico Vittorio for an enjoyable collaboration, and the conveners of track 01 for organizing stimulating sessions.

References

[1] M. Cavan-Piton, D. Guadagnoli, M. Oertel, H. Seong and L. Vittorio, *Axion Emission from Strange Matter in Core-Collapse SNe*, *Phys. Rev. Lett.* **133** (2024) 121002, [2401.10979].

[2] H. Georgi, D. B. Kaplan and L. Randall, *Manifesting the Invisible Axion at Low-energies*, *Phys. Lett. B* **169** (1986) 73–78.

[3] G. G. Raffelt, *Astrophysical methods to constrain axions and other novel particle phenomena*, *Phys. Rept.* **198** (1990) 1–113.

[4] A. Caputo and G. Raffelt, *Astrophysical Axion Bounds: The 2024 Edition*, in *1st Training School of the COST Action COSMIC WISPers (CA21106)*, 1, 2024. 2401.13728. DOI.

[5] P. Carenza, T. Fischer, M. Giannotti, G. Guo, G. Martínez-Pinedo and A. Mirizzi, *Improved axion emissivity from a supernova via nucleon-nucleon bremsstrahlung*, *JCAP* **10** (2019) 016, [1906.11844].

[6] P. Carenza, B. Fore, M. Giannotti, A. Mirizzi and S. Reddy, *Enhanced Supernova Axion Emission and its Implications*, *Phys. Rev. Lett.* **126** (2021) 071102, [2010.02943].

[7] J. Martin Camalich, M. Pospelov, P. N. H. Vuong, R. Ziegler and J. Zupan, *Quark Flavor Phenomenology of the QCD Axion*, *Phys. Rev. D* **102** (2020) 015023, [2002.04623].

[8] M. Marques, M. Oertel, M. Hempel and J. Novak, *New temperature dependent hyperonic equation of state: Application to rotating neutron star models and I-Q relations*, *Phys. Rev. C* **96** (2017) 045806, [1706.02913].

[9] M. Fortin, M. Oertel and C. Providência, *Hyperons in hot dense matter: what do the constraints tell us for equation of state?*, *Publ. Astron. Soc. Austral.* **35** (2018) 44, [1711.09427].

[10] M. Buschmann, C. Dessert, J. W. Foster, A. J. Long and B. R. Safdi, *Upper Limit on the QCD Axion Mass from Isolated Neutron Star Cooling*, *Phys. Rev. Lett.* **128** (2022) 091102, [2111.09892].